PEGylation Promotes Hemoglobin Tetramer Dissociation

PEGylation Promotes Hemoglobin Tetramer Dissociation

Dario Caccia,[†,‡] Luca Ronda,[†,||] Raffaella Frassi,[‡] Michele Perrella,[‡] Elena Del Favero,[§] Stefano Bruno,[||] Barbara Pioselli,[||] Stefania Abbruzzetti,[⊥] Cristiano Viappiani,[⊥] and Andrea Mozzarelli*[,||,#]

Dipartimento di Scienze e Tecnologie Biomediche, Dipartimento di Chimica, Biochimica e Biotecnologie per la Medicina, Università degli Studi di Milano, and LITA (Laboratorio Interdisciplinare di Tecnologie Avanzate), 20090 Segrate, Milano, Italy, and Dipartimento di Biochimica e Biologia Molecolare, Dipartimento di Fisica, Università di Parma, and NEST CNR-INFM, Istituto Nazionale di Biostrutture e Biosistemi, 43100 Parma, Italy. Received March 26, 2009; Revised Manuscript Received May 19, 2009

Hemoglobin conjugated with poly(ethylene glycol) (PEG) acts as an oxygen carrier free in plasma, substituting red blood cells in supplementing oxygen in hypo-oxygenation pathologies. Given the complexity of oxygen delivery controls, subtle structural and functional differences in PEGylated hemoglobins might be associated with distinct physiological responses and, potentially, adverse effects. We have compared hemoglobin PEGylated under anaerobic conditions, called PEG-Hb^{deoxy}, with hemoglobin PEGylated under aerobic conditions, called PEG-Hb^{oxy}, a product that mimics Hemospan, produced by Sangart, Inc. SDS PAGE and MALDI-TOF analyses demonstrated that PEG conjugation yields products characterized by a broad distribution of PEG/hemoglobin ratios. The elution profiles in size-exclusion chromatography indicate that both products exhibit a more homogeneous distribution of molecular weight/hydrodynamic volume under deoxy conditions and at higher concentrations. PEG-Hb^{oxy} shows high oxygen affinity, low modulation of allosteric effectors, almost no cooperativity, a fast and monophasic CO binding, and a limited dependence of functional properties on concentration, whereas PEG-Hb^{deoxy} exhibits oxygen binding curves that significantly depend on protein concentration, and a slow CO binding, similar to native hemoglobin. PEGylated CO-hemoglobins, probed by flash photolysis, exhibited a lower amplitude for the geminate rebinding phase with respect to native hemoglobin and a negligible T state bimolecular CO rebinding phase. These findings are explained by an increased dissociation of PEGylated hemoglobins into dimers and perturbed T and R states with decreased quaternary transition rates. These features are more pronounced for PEG-Hb^{oxy} than PEG-Hb^{deoxy}. The detected heterogeneity might be a source of adverse effects when PEGylated Hbs are used as blood substitutes.

Hemoglobin-based oxygen carriers (HBOC)[1] (*1*−*4*) are potential therapeutic agents for clinical needs that cannot be fullfilled by blood transfusions, such as (i) acute hemorrhages associated with accidents or weapon wounds in location far from hospitals, (ii) immunoreactivity against all red blood cell determinants, (iii) oxygen supply to patients that do not accept blood transfusions for religious dictates, (iv) oxygenation of ischemic tissues where red blood cells cannot diffuse (*5, 6*), and (v) increase in oxygen concentration in solid tumors for the improvement of radiation therapy (*7, 8*). Moreover, HBOCs can be used for (i) partial substitution of normal transfusion to save blood units during orthopedic surgeries, (ii) reduction of the exposure of preterm infants to adult red cells, potentially causing severe chronic pathologies (*9*), and (iii) safe supply of an oxygen supplier in world countries where blood units from healthy donors are limited. The absence of cross-matching, the room temperature storage, the more than one year shelf life, and the possibility of tuning hemoglobin (Hb) oxygen affinity depending on clinical requirements are other advantages for HBOCs with respect to red blood cell transfusions. Several products have been developed based on approaches aimed at increasing the molecular size of Hb via either subunit cross-linking (*10*−*14*) or conjugation with poly(ethylene glycol) (PEG) (*15*−*18*) to avoid vessel extravasation and renal ultrafiltration. Only a few of these products, manufactured by companies, have progressed and been evaluated in phase II and III trials (*12, 19*−*22*). So far, no products have been approved by the FDA. Moreover, a meta-analysis of the recent clinical trials has evidenced that, to some extent, all products cause medium to severe adverse effects, such as death, myocardial infarction, and pancreatitis (*23*), strongly questioning their safe use. However, companies have expressed concerns on the validity of the meta-analysis (*24, 25*).

It should be fully appreciated that HBOC is a peculiar drug because the amount of product that is injected into the plasma is on the order of grams in comparison to milligrams or micrograms for most other drugs. Thus, even a small amount

* Corresponding author. Andrea Mozzarelli, Dipartimento di Biochimica e Biologia Molecolare, Università di Parma, Viale G.P. Usberti 23/A, 43100 Parma, Italy. Fax 39-0521-905151. E-mail: andrea.mozzarelli@unipr.it.

[†] These two authors contributed equally to the work.

[‡] Dipartimento di Scienze e Tecnologie Biomediche, Università degli Studi di Milano.

[§] Dipartimento di Chimica, Biochimica e Biotecnologie per la Medicina, Università degli Studi di Milano.

[||] Dipartimento di Biochimica e Biologia Molecolare, Università di Parma.

[⊥] Dipartimento di Fisica, Università di Parma, and NEST CNR-INFM.

[#] Istituto Nazionale di Biostrutture e Biosistemi.

[1] Abbreviations: ACN, acetonitrile; $C_{12}E_8$, octaethylene glycol monododecyl ether; DLS, dynamic light scattering; 2,3-BPG, 2,3-diphophoglycerate; Hb, hemoglobin; HBOC, hemoglobin-based oxygen carrier; IHP, inositol hexaphosphate; IMT, 2-iminothiolane; MAL-PEG, maleimidoethyl poly(ethylene glycol); MS, mass spectroscopy; M_r, relative molecular mass; *n*, Hill's cooperativity coefficient; NEM, *N*-ethylmaleimide; NES-Hb, hemoglobin thiolated and treated with NEM under anaerobic conditions; ODC, oxygen dissociation curve; PEG, poly(ethylene glycol); PEG-BSA, PEGylated bovine serum albumin; PEG-Hb, PEGylated hemoglobin, PEG-Hb^{deoxy} and PEG-Hb^{oxy}, hemoglobin thiolated and PEGylated under anaerobic and aerobic conditions, respectively; SLS, static light scattering; TFA, trifluoro acetic acid.

10.1021/bc900130f CCC: $40.75
Published on Web 06/17/2009

Table 1. Biochemical Characterization of Hb Derivatives[a]

species	reaction cycles	total SH	free SH	conjugation (NEM or MAL-PEG)
HbA	–	–	2.3	–
NEM-Hb	2 cycles IMT+NEM	7.7	2.3	5.3 (NEM)
PEG-Hb^{deoxy}	1 cycle IMT+MAL-PEG	9.0	2.3	6.7 (MAL-PEG)
PEG-Hb^{oxy}	1 cycle IMT+MAL-PEG	6.9	1.0	5.9 (MAL-PEG)
PEG-BSA	1 cycle IMT+MAL-PEG	5.9	0.2	5.7 (MAL-PEG)

[a] IMT-modified amino groups before (total SH) and after reaction with NEM or MAL-PEG (free SH) as determined on a tetramer basis by thiol titration with the method of Ampulsky et al. (*39*) The number of residues conjugated with NEM or MAL-PEG was equal to the difference between total SH and free SH. The titre of Cysβ93 of native Hb yielded by the method was 2.3.

of byproduct and heterogeneity generated by the chemical procedures or slight deviation of the functional properties from the physiological needs might be responsible for some of the observed adverse effects. However, so far, no investigation has been carried out to link structural and functional properties of products with the observed adverse effects. One of these products, MP4, trade name Hemospan, is obtained via the conjugation of Hb with an average of 6−7 PEG 5000 (M_r) chains under oxygenated conditions in a two-step procedure: first, oxyHb is thiolated by treatment with iminothiolane (IMT), and then, thiols react with the PEG-maleimido derivative MAL-PEG (*16, 26*). Hemospan has completed phase III clinical trials to test its capacity for prevention and treatment of hypotension during orthopedic surgery (*22, 25, 27*). Hemospan exhibits high oxygen affinity and low cooperativity, which makes it more similar to Hb dimers than to the physiological tetrameric oxygen carrier. These features might have originated from the interference of PEG molecules with Hb amino groups of the organic phosphate binding pocket and the sulfhydryl groups of Cysβ93 (*28−31*), which are involved in NO binding (*16, 32, 33*). Recently, it was also demonstrated that PEGylated Hb exhibits an increase in the nitrite reductase activity (*31*).

With the aim of protection from PEGylation function-associated groups, PEGylation of Hb was carried out under anaerobic conditions, in the presence of IHP and Cl^- (*34*). This PEGylated Hb exhibits lower oxygen affinities than Hemospan and normal or moderately reduced response to 2,3-BPG, and retains about 50% of the cooperativity of native Hb (*34, 35*). Otherwise, in transfused rats, retention time, renal filtration, and pressure effects of Hb, PEGylated under anaerobic conditions with seven PEG and seven propionyl groups, called Euro PEG-Hb, were found to be similar to those observed for Hb PEGylated under aerobic conditions (*35*). The altered oxygen affinity and cooperativity of the PEGylated products might not be due solely to lysines modifications. It is known that interface mutants or chemically modified Hbs characterized by an increased oxygen affinity and reduced cooperativity exhibit perturbed tetramer−dimer equilibria, favoring the latter species (*36, 37*). This might also be the effect of PEGylation on Hb.

In the perspective of the use of PEGylated Hb products as a blood substitute and in light of the recently observed adverse effects (*25*), we have carried out a detailed comparison of the structural and functional properties between a product prepared using the procedure reported for Hemospan (*16, 26*), that we named PEG-Hb^{oxy}, that is conjugated with six PEG molecules under aerobic conditions, and Hb, similarly modified with an average of six PEG molecules, under anaerobic conditions, that we named PEG-Hb^{deoxy}. We have studied the molecular weight distribution, physicochemical properties, oxygen binding curves, and time courses of CO binding as a function of protein concentrations, in the absence and presence of allosteric effectors. Results were correlated with elution profiles in size exclusion chromatography under deoxygenated and oxygenated conditions. Our studies suggest that PEG-Hb^{oxy} more than PEG-Hb^{deoxy} exhibits altered tetramer−dimer equilibria, due to slower association rates of the PEGylated dimers as compared with native Hb, thus accounting for most of the observed distinct functional properties. This conclusion is in keeping with a very recent study carried out on Hb PEGylated at both Valα1 and Valβ1 (*38*).

EXPERIMENTAL PROCEDURES

Materials. IMT, IHP, NEM, molecular weight markers, BSA, and MALDI calibration kit were purchased from Sigma Aldrich. Reagents and equipment for SDS-PAGE were from Biorad Laboratories Inc. Ultrafiltration membranes and kits were from Sartorius Stedim and Millipore. MAL-PEG (molecular mass 5.6 kDa) was from Nektar Molecule Engineering (Nektar Therapeutics).

Protein Modification. Conjugated Hbs were prepared by treating HbA in 50 mM Na-phosphate, 100 mM NaCl, 0.5 mM EDTA, pH 7 at 20 °C, with an excess of IMT and MAL-PEG, or NEM, under anaerobic conditions in the presence of IHP, as previously described (*34*) to produce PEG-Hb^{deoxy}. The amount of IMT and the reaction time were adjusted to achieve the desired degree of thiolation and, thus, the number of conjugated PEG molecules. Concentrated and deoxygenated lysine and cysteine solutions were added to stop IMT and MAL-PEG reactions, respectively. PEG-Hb^{deoxy} was then equilibrated with 100 mM NaCl by seven ultrafiltration cycles, under aerobic conditions, at 5 °C, using a 30 kDa cutoff Amicon membrane. The solution was concentrated to one-third of the initial volume before redilution with NaCl solution. The number of conjugated PEG chains was estimated by treating deoxy Hb with IMT under the same conditions without the addition of MAL-PEG. The thiol titer determined by a biochemical method (*39*), corrected for the titer determined after treatment with MAL-PEG, or NEM, yielded the number of conjugated PEG/tetramer, or NEM/tetramer (*34*). PEG-Hb^{oxy} was prepared as described by Vandegriff et al. (*16*). Hb, PEG-Hb^{deoxy}, and PEG-Hb^{oxy} were stored in liquid nitrogen. The ferric Hb content was <2%. Hb concentration is expressed on a heme basis. BSA (68 kDa, 59 lysines) was PEGylated under aerobic conditions by the same procedure described for PEG-Hb^{deoxy} to obtain a protein conjugated with an average number of 6 PEG/molecule. Since the BSA sample was contaminated by 5% IgG immunoglobulin, the product was also contaminated by PEGylated IgG, which showed up in size exclusion chromatography as an inflection of the leading edge of the elution profile of PEG-BSA. The characteristics of the various preparations are summarized in Table 1.

SDS-PAGE and Protein Extraction. SDS-PAGE was carried out according to Laemli (*40*) using acrylamide and piperazine diacrylylamide as the cross-linker. Gels were stained with BioSafe G-250 Coomassie Brilliant Blue compatible with MS analysis and scanned using Quantity One software. Protein bands were excised from the gels and destained with a 40/10 (v/v) mixture of methanol/acetic acid. The proteins were recovered by passive elution at 37 °C using the SDS-PAGE running buffer and concentrated by Vivaspin 2 (Sartorius) centrifugal concentrators, which facilitates SDS removal.

Mass Spectrometry. A layer of sinapinic acid in acetone was spotted onto the sample well before adding 1 μL protein aliquotes diluted with matrix solution containing 30 mg/mL sinapinic acid in 50/50 (v/v) ACN/0.1% TFA. MALDI TOF mass spectra were obtained using a MALDI-LR mass spectrometer (Waters Italia) operated in negative linear mode. External calibration was carried out in the 7−70 kDa mass range using protein standards from the ProteoMass Peptide and Protein MALDI-MS Calibration kit: apomyoglobin (equine) ($M+H^+$: 16 952.27), aldolase ($M+H^+$: 39 212.28), albumin ($M+H^+$: 66 430.09) and High Mass Post Acceleration Linear detector to increase the sensitivity for the PEGylated molecules.

Static and Dynamic Light Scattering. Laser light scattering was carried out with a goniometer (BI-200SM Brookhaven Instrument Corporation) equipped with a BI9K Digital correlator and a solid-state 676 nm light source. Independent SLS and DLS measurements were carried out at 20 °C, under aerobic conditions, on Hb, PEG-Hb^{deoxy}, and PEG-Hb^{deoxy} in a solution containing 50 mM Na-phosphate, 100 mM NaCl, 0.5 mM EDTA, 0.5 mM NaCN, pH 7, at 40−280 μM concentration range. The hydrodynamic radii were determined by Cumulant and Fourier Transform analysis of the intensity correlation function measured by DLS (*41*). Independent SLS measurements provided information about the average molecular weight and concentration of macromolecules after absolute intensity calibration with a 0.02 mg/mL $C_{12}E_8$ solution (*42*).

Size Exclusion Chromatography. Chromatography was carried out in 50 mM Na-phosphate, 100 mM NaCl, 0.5 mM EDTA, pH 7, with an AKTA Prime instrument and a HiLoad Superdex 200 column (≈120 mL bed volume, 600 kDa mass exclusion limit), thermostatted at 20 °C, at flow rate of 1.5 mL/min (Amersham Pharmacia Biotech). The retention time was 40−70 min using 0.5 mL samples of PEGylated Hb. To carry out anaerobic chromatography, the buffer reservoir was kept under nitrogen and 1 mM Na-dithionite was added to the buffer. Samples were loaded after deoxygenation by nitrogen tonometry and addition of Na-dithionite. The eluate from Hb chromatographic analysis was monitored at 436 nm to avoid dithionite interference, whereas the flowthrough of BSA chromatographic analysis was monitored at 280 nm. Chromatograms were normalized to absorbance values versus molecular mass derived from standard proteins calibration.

To determine the tetramer−dimer equilibrium constant of oxy Hb and oxy NES-Hb, a HiLoad Sephacryl S-200 column was used (bed volume ≈79 mL, matrix volume ≈3 mL, according to the manufacturer specifications, and void volume ≈38 mL, as determined by Blue Dextran, 250 kDa mass exclusion limit). Solute saturation was achieved by loading 15 mL samples. The column was run at 0.5 mL/min flow rate at 20 °C. A solute in rapid tetramer−dimer equilibrium, as Hb, loaded on such a column under solute saturating conditions, shows an elution profile characterized by a plateau region between a leading and a trailing edge. The solute elution volume at the inflection point of the leading edge, V, is related to the fraction of dissociated tetramers, α, through eq 1 (*43*):

$$V = V_0 + [\sigma_T + \alpha(\sigma_D - \sigma_T)]V_i \quad (1)$$

where V_0 is the void volume, V_i the internal matrix volume, provided by the manufacturer, and σ_T and σ_D are parameters that characterize the matrix interactions with tetramers and dimers, respectively. These parameters were obtained using enough high and low Hb concentrations to justify the assumption that the protein was in tetrameric and dimeric form, respectively. The gradient of the elution profile was analyzed to precisely determine the elution volume at the inflection point of the leading edge. The dissociation constant is related to α through eq 2:

$$K_d = \alpha^2 C/(1 - \alpha) \quad (2)$$

where C is the solute plateau concentration. Under deoxy conditions, the method could not be used since both normal and NES-Hb require dilution much beyond the limit of concentration detection of the technique and the tetramer−dimer equilibration is not rapid relative to the time scale of the chromatographic run.

Oxygen Affinity Measurements. Oxygen dissociation curves (ODCs) as a function of protein concentration were carried out at 15 °C in a solution containing the enzymatic metHb reducing system (*44*), at pH 7.0, using a novel homemade apparatus (*45*). The gas mixture generated by Environics 200 and 4000 (Environics, Inc.) flows in a thermostatted humidifier and then in the sample chamber consisting of a 2 mm optical path cuvette fused to a 25 mL open-top threaded reservoir with fittings for inlet and outlet gas lines. The chamber is thermostatted in a shaking bath. The sample compartment of a CARY 400 spectrophotometer (Varian, Inc.) is also thermostatted. Fractional oxygen saturations and oxidized hemes were determined by fitting the observed spectra to a linear combination of reference spectra (*46, 47*). ODCs of PEG-Hb^{deoxy}, in the absence of allosteric effectors, at different protein concentrations, were globally fitted using eq 3, assuming two independent species ***a*** and ***b***, characterized by $p50_a$ and Hill coefficient n_a, and $p50_b$ and Hill coefficient n_b, respectively, varying only the relative fraction of species ***a***, f_a, as a function of concentration:

$$Y = f_a \frac{pO_2^{na}}{pO_2^{na} + p50_a^{na}} + (1 - f_a) \frac{pO_2^{nb}}{pO_2^{nb} + p50_b^{nb}} \quad (3)$$

ODCs in the presence of the allosteric effectors Cl^- and CO_2 were fitted with eq 1, constraining $p50_a$ and n_a to be equal to those calculated in the absence of allosteric effectors. It was assumed that functional properties of species ***a*** are unaffected by effectors because this species corresponds to Hb dimers, whereas functional properties of species ***b*** are affected because this species corresponds to Hb tetramers (see Results). ODCs of PEG-Hb^{oxy} and Hb were fitted to a single species characterized by p50 and Hill coefficient n.

CO Binding Kinetics. CO binding to HbA, PEG-Hb^{deoxy}, and PEG-Hb^{oxy} was followed by stopped-flow apparatus (SX.18 MV, Applied Photophysics) at a single wavelength (435 nm). Two millimolar Na-dithionite was added to deoxygenated protein and ligand solutions to completely remove oxygen. Depending on Hb concentration, a path length of 0.2 or 1 cm was used.

Flash photolysis experiments were performed with a setup described elsewhere (*48, 49*), following the absorbance change at 436 nm. Photolysis yields for all species were evaluated and found to be similar. The rebinding kinetic traces were first converted to fraction of deoxy-protein as a function of time. The lifetime distribution associated with the observed CO rebinding kinetics was evaluated using the program MemExp (version 3.0) (*50*). The program MemExp uses a maximum entropy method (MEM) and either nonlinear least-squares (NLS) or maximum likelihood (ML) fitting to analyze a general time-dependent signal in terms of distributed and discrete lifetimes. A distribution of effective log-lifetimes, $g(\log(\tau))$, was extracted from the data without restriction to any functional form, as previously described (*51−53*).

Stopped-flow and flash photolysis experiments were carried out in a solution containing 1 atm CO, 100 mM Hepes, 1 mM EDTA, pH 7.0, at 15 °C.

RESULTS

Analysis of PEGylated Hbs by SDS-PAGE and Mass Spectrometry. A previous mass spectrometry (MS) study of Hb PEGylated under anaerobic conditions showed that 5 lysines

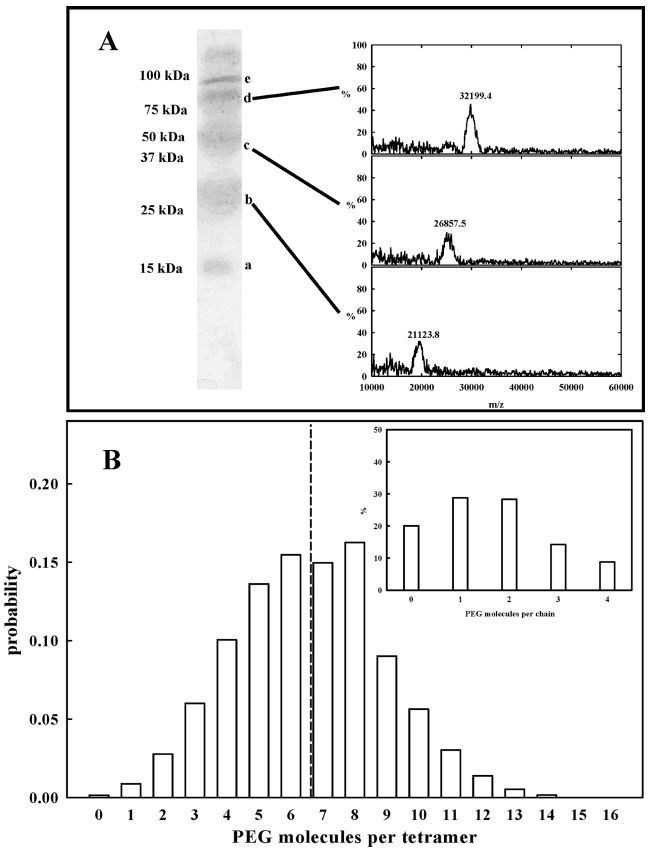

Figure 1. PEG-Hb^{deoxy} heterogeneity. (A) SDS-PAGE and molecular weight determination by MALDI-TOF of PEGylated Hb products. PEG-Hb^{deoxy} was separated by SDS-PAGE (left panel). The molecular weight of species ***a*** was 16 kDa, according to molecular weight markers (not shown). The *m*/*z* values of the species extracted from bands b, c, and d and analyzed by MALDI-TOF MS (right panel) were 21123, 26857, 32199, respectively, indicating the addition of 1, 2, and 3 5.6 kDa PEG molecules. (B) Distribution of unmodified and PEGylated species in a sample of PEG-Hb^{deoxy} calculated from the relative amounts of the various chains determined in Figure 1A. Relative proportions of unmodified and PEGylated chains, as determined by the analysis of the intensities of the stained bands of the SDS-PAGE separations, are reported in Figure 1B, inset.

per subunit were modified by IMT at a significantly higher rate than three additional lysines, both on the α and β chains (*34*). The reactivity differences between these 5 reactive lysines do not allow the preparation of a homogeneous product. Only 6−7 residues per tetramer are PEGylated, showing a significant population of unmodified chains that suppressed the ionization of PEGylated chains in MALDI-TOF MS, thus yielding only a qualitative information on the presence of non-PEGylated Hb chains (*34*). To obtain a quantitative estimate of the proportion of unmodified vs PEGylated tetramers, PEG-Hb^{deoxy} was characterized by SDS-PAGE, which was proven effective in separating nonconjugated and conjugated Hb chains (Figure 1A, left panel). A similar study has recently been carried out for Hemospan (*26*). Since the species in band a runs as HbA chains (data not shown), it was assumed that this species corresponds to the unmodified globin chains. Bands b, c, d, and e migrate with an apparent molecular weight of approximately 25, 45, 75, and 90 kDa, respectively, as calculated using protein molecular weight standards. The species extracted from the bands were individually characterized by MALDI-TOF MS, as shown in Figure 1A, right panel. Bands b, c, and d were assigned to globin chains conjugated with one, two, and three 5.6 kDa PEG molecules, respectively. The protein recovery from the low-intensity band e was not sufficient to collect reliable data in MALDI TOF analysis. However, it is reasonable to assume that this component is conjugated with four PEG molecules per globin chain. The tetramer distribution as a function of the number of conjugated PEG molecules (Figure 1B) was calculated using the densitometric analysis of the stained protein bands (Figure 1B, inset). It displays a wide distribution, spanning from unmodified to 12 PEG molecules per tetramer. The weighted mean is 6.6 PEG molecules/tetramer, in good agreement with the biochemical estimation (see Experimental Procedures, Table 1). Such a distribution indicates that, under these conditions, a wide variety of PEGylated Hb species is present and the probability to find either unmodified or highly PEGylated tetramers (>12−13 PEG molecules) is negligible. Furthermore, samples of PEG-Hb^{oxy} and PEG-Hb^{deoxy} were analyzed by native gel electrophoresis (data not shown). The densitometric profiles indicate that both PEG-Hb^{oxy} and PEG-Hb^{deoxy} are heterogeneous products (see also ref 26).

Analysis of PEGylated Hbs by Static and Dynamic Light Scattering. Solutions containing HbA, PEG-Hb^{oxy}, and PEG-Hb^{deoxy}, at a concentration of 40−280 μM, were characterized by static light scattering (SLS) and dynamic light scattering (DLS) measurements. The observed weight average molecular masses were 68 ± 5, 105 ± 2, and 99 ± 1 kDa, respectively. The average number of PEG chains per tetramer, 6.6 (PEG-Hb^{deoxy}) and 5.6 (PEG-Hb^{oxy}), calculated from these mass values agreed with the values obtained by the biochemical characterization and mass spectroscopy measurements (Table 1). The average hydrodynamic diameters of HbA, PEG-Hb^{deoxy}, and PEG-Hb^{oxy} were 59, 105, and 104 Å, respectively, within 5% error. Using the static and dynamic measurements, it was calculated that Hb hydrodynamic radius agreed with the dimension of a globular particle with 66 kDa molecular mass. In the case of PEG-Hb^{deoxy} and PEG-Hb^{oxy}, PEGylation brought about a significant increase in hydrodynamic radius with respect to the increase in the molecular mass, suggesting a Hb core surrounded by a 15−20 Å thick shell of highly hydrated flexible PEG monomers.

Analysis of PEGylated Hbs by Size Exclusion Chromatography. Column chromatography of oxy Hb and oxy NES-Hb, at 20 °C in 50 mM phosphate, 100 mM NaCl, 0.5 mM EDTA, 0.1 mM NaCN, pH 7, under aerobic conditions and protein column saturation, yielded single plateau regions at all protein concentrations in the 4−4000 μM range. The averaged dimer/tetramer $K_{d(oxy)}$ values were 0.26 ± 0.08 and 0.42 ± 0.07 μM, respectively, comparable to published values of 0.48−1.9 μM for liganded human Hbs under similar conditions (*36, 37*). Under anaerobic conditions, the dimer/tetramer $K_{d(deoxy)}$ values of deoxy NES-Hb could not be obtained by this approach due to the extremely low value of the equilibrium dissociation constant, as already known for Hb (*54*).

The chromatography of PEG-Hb^{deoxy} and PEG-Hb^{oxy}, under aerobic conditions, failed to yield a single plateau because of either the heterogeneity of the PEGylated proteins or the slow equilibration of the species during chromatography. To clarify this issue, we carried out size exclusion chromatography using nonsaturating column conditions. Oxy Hb at all concentrations was eluted as a single, nearly symmetrical peak, which shifted from 65 ± 3 kDa at 800 μM to lower values upon dilution due to the increased fraction of dimers in rapid equilibrium with tetramers (data not shown). Deoxy Hb was eluted as a single, 65 kDa symmetrical peak at all concentrations (data not shown). Chromatography of PEG-BSA (Figure 2A, inset) showed a single main peak with an inflection in the leading edge due to the presence of PEGylated IgG immunoglobulin. This clearly indicates that under the conditions of the chromatography the molecular sieve could not resolve species differing in the number of conjugated PEG chains. However, a shift in the apparent molecular weight from 540 ± 25 to 640 ± 25 kDa occurred

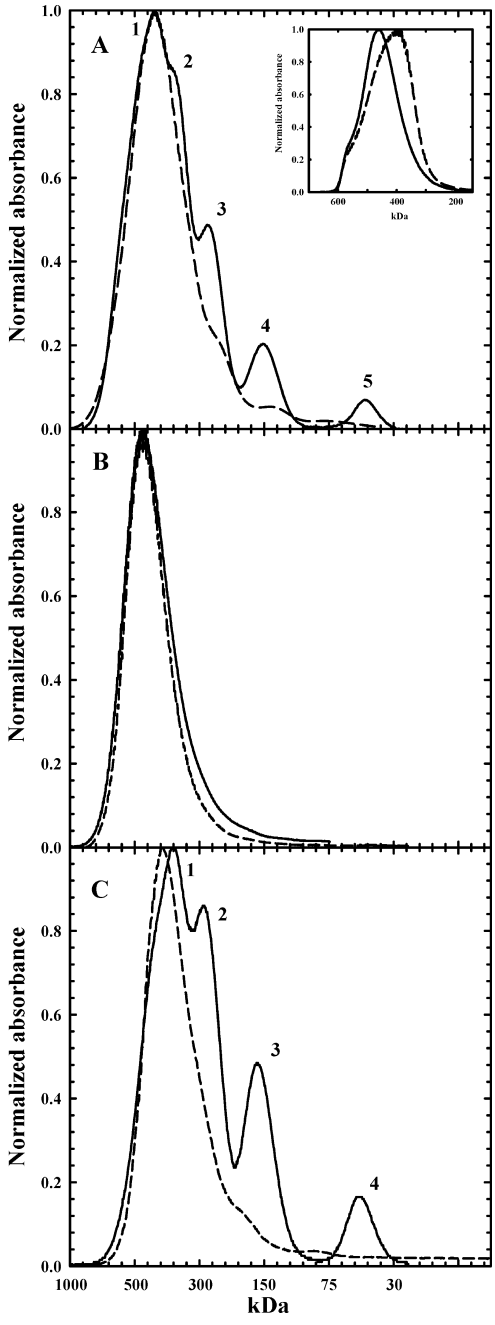

Figure 2. Size exclusion chromatography. A HiLoad Superdex 200 column (about 120 mL bed volume) was equilibrated at 20 °C with 50 mM Na-phosphate, 100 mM NaCl, 0.5 mM Na-EDTA, 0.1 mM NaCN, pH 7. Samples (0.5 mL) were eluted at a 1.5 mL/min flow rate. The elution volumes in the abscissa were transformed into molecular weight units (kDa) by column calibration using known standards. Absorbance values on the ordinate were normalized to the highest value. (A) (dash line) 800 and (solid line) 8 μM oxy PEG-Hb^{deoxy}. The species eluted in peaks 1−5 were not identified. The apparent molecular weight of peak 1 is 460 kDa. Inset: 800 μM (solid line) and 8 μM (dash line) PEG-BSA. The apparent molecular weights are 540 and 640 kDa, respectively. The inflection of the leading edge indicates the presence of PEGylated IgG, which contaminated the native BSA sample (5%). (B) 8 μM deoxy PEG-Hb^{deoxy} in the presence of 1 mM Na-dithionite. (dash line), sample prepared by dilution of a deoxygenated 800 μM solution. (solid line), sample prepared by Na-dithionite addition to a 8 μM oxygenated solution. The apparent molecular weight of the peak is 500 kDa. (C) 8 μM PEG-Hb^{oxy} under aerobic (solid line) and anaerobic (dash line) conditions. The species in peaks 1−4 were not identified. The apparent molecular weight of peak 1 is 380 kDa. The 8 μM deoxy PEG-Hb^{oxy} sample was obtained by the addition of Na-dithionite to a 8 μM oxygenated sample before loading. The apparent molecular weight of the peak is 430 kDa.

upon dilution (Figure 2A, inset), due to non-ideality of the solute−matrix interactions. The non-ideality effect was also observed using Hb at high concentrations where dissociation into dimers is not significant (data not shown). At 800 μM concentration, oxy PEG-Hb^{deoxy} was eluted as a main species with an apparent molecular weight of 460 ± 25 kDa, more than four times the value calculated on the basis of the average PEG/tetramer number (Figure 2A). A trailing edge, however, indicated the presence of small amounts of other components. At 2 μM concentration, four additional unidentified components, partially or completely resolved, were observed (Figure 2A). The formation of low relative molecular mass (M_r) components upon dilution was reversible, since a 8 μM sample of oxy PEG-Hb^{deoxy} reconcentrated to 800 μM was eluted as the original undiluted 800 μM sample (data not shown). PEG-Hb^{deoxy} chromatography under anaerobic conditions, at all concentrations, yielded a single peak with an apparent molecular weight of 500 kDa. However, the slight trailing observed with diluted samples depended on the modality of sample dilution. When a 800 μM oxygenated sample was deoxygenated before dilution to 8 μM, trailing was minimal (Figure 2B). If dilution to 8 μM was carried out under aerobic conditions followed by rapid deoxygenation with Na-dithionite, trailing was more pronounced (Figure 2B). Under aerobic conditions and at 8 μM concentration (Figure 2C), PEG-Hb^{oxy} showed at least a five-component elution pattern with the main component, **1** (Figure 2C), shifted to an apparently lower molecular weight (380 kDa) than component **1** in the PEG-Hb^{deoxy} elution pattern, Figure 2A, and a significant increase in the relative proportions of partially or completely resolved species as compared with PEG-Hb^{deoxy} under the same conditions (Figure 2C). Under anaerobic conditions and when rapid deoxygenation of 8 μM oxy PEG-Hb^{oxy} was carried out by Na-dithionite addition (Figure 2C), the apparent M_r of the main peak was 430 kDa and the presence of incompletely reassociated species was more evident than in the case of PEG-Hb^{deoxy} (Figure 2B).

Oxygen Binding Curves of PEG-Hb^{deoxy} and PEG-Hb^{oxy} as a Function of Protein Concentration, in the Absence and Presence of Allosteric Effectors. ODCs were carried for PEG-Hb^{deoxy} at protein concentrations between 11 and 550 μM, for PEG-Hb^{oxy} at 219 μM and for HbA at 13 and 193 μM in a solution containing 100 mM Hepes, 1 mM EDTA, pH 7, at 15 °C (Figure 3). The apparent oxygen affinity for PEG-Hb^{deoxy} was found to increase as protein concentration decreased. ODCs were globally fitted to two components, ***a*** with p50$_a$ = 0.80 ± 0.12 Torr and n_a = 1.33 ± 0.09 and ***b*** with p50$_b$ = 3.18 ± 0.08 Torr and n_b = 2.54 ± 0.19. The fraction of species ***a***, f_a, decreases with increasing Hb concentration, remaining constant above 200 μM (Figure 3, inset). The dependence of f_a on Hb concentration was fitted to a binding isotherm with a dissociation constant K_d of 21.5 ± 2.3 μM.

ODCs for HbA (Figure 3) do not exhibit variation as a function of protein concentration and were fitted to an equation for a single oxygen binding species with a p50 of 2.65 ± 0.02 Torr and Hill n of 2.39 ± 0.05, values very close to those exhibited by species ***b***. ODC for PEG-Hb^{oxy} (Figure 3) was well fitted to a single species with p50 of 0.66 ± 0.03 Torr and Hill n of 1.36 ± 0.03, values very close to those exhibited by species ***a***. However, when ODCs were measured for PEG-Hb^{oxy} fractions separated by native PAGE (data not shown), p50 values were found to even 2-fold different between them.

PEGylated Hbs obtained under anaerobic conditions exhibited nearly normal oxygen affinity modulation by 2,3-BPG, due to the organic phosphate binding pocket protection by IHP during the chemical modification and a Bohr effect reduced by 20−25% (*34*). However, more relevant in view of the use of PEG-Hbs as HBOC are the effects of CO_2 and Cl^-, which are allosteric

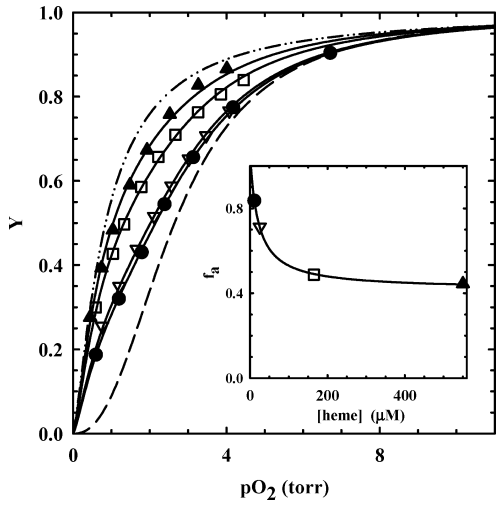

Figure 3. Concentration dependence of oxygen binding to PEG-Hb^{deoxy}, PEG-Hb^{oxy}, and Hb. ODCs at 11 (closed up-triangles), 25 (open squares), 165 (open down-triangles), and 550 μM (closed circles) concentrations of PEG-Hb^{deoxy} were determined in 100 mM Hepes, 1 mM EDTA, pH 7, at 15 °C. ODCs were determined under the same conditions for 193 μM HbA (dash line) and 219 μM PEG-Hb^{oxy}. (dash-dot-dot line). ODCs for PEG-Hb^{deoxy} were globally fitted (solid lines) assuming different fractions of component **a** ($p50_a = 0.80$ Torr and $n_a = 1.33$) and **b** ($p50_b = 3.18$ Torr, $n_b = 2.54$). HbA and PEG-Hb^{oxy} were fitted to a single species with p50 of 2.61 ± 0.05 Torr and Hill n of 2.36 ± 0.06 and p50 of 0.85 ± 0.02 Torr and Hill n of 1.34 ± 0.04, respectively. Inset: dependence of the fraction of component **a** on concentration. The dependence was fitted to a binding isotherm with an apparent tetramer−dimer equilibrium constant $K_d = 21.5 \pm 2.3$ μM.

effectors present in the plasma. The comparison of p50 and Hill n values for Hb, NES-Hb, PEG-Hb^{deoxy}, and PEG-Hb^{oxy}, in the absence and presence of physiological concentrations of CO_2 and saturating concentration of Cl^- (Table 2), shows a decrease in oxygen affinity brought about by the allosteric ligands on both PEGylated Hbs, although to an extent that is less than on HbA.

CO Binding Kinetics to HbA, PEG-Hb^{deoxy}, and PEG-Hb^{oxy}. Binding kinetics of CO to HbA is characterized by an autocatalytic behavior due to the shift of the quaternary T to R state equilibrium as a function of ligand saturation (*55, 56*). The observed log rate constants, expressed as M^{-1} s^{-1} of 0.5 atm CO binding to Hb, determined by stopped-flow measurements (Figure 4), were 5.034 ± 0.001 and 5.776 ± 0.008 at 107 μM HbA, and only slightly higher (5.101 ± 0.002 and 5.782 ± 0.009) at 3.5 μM HbA, in good agreement with previously determined values (*57*). The kinetics of CO binding to 96 and 14 μM PEG-Hb^{oxy} (Figure 4) were monophasic with a log rate constant of ~5.3, independent of protein concentration. The CO binding kinetics to 88 and 6.6 μM PEG-Hb^{deoxy} (Figure 4) were nearly monophasic with log rate constants of 5.073 ± 0.001 and 5.120 ± 0.001, respectively.

The kinetic trace of CO rebinding to HbA after laser flash photolysis (Figure 5A) originates from three distinct processes: a nanosecond geminate rebinding of CO still present in the heme pocket of R state molecules that have not yet relaxed to the T state, a microsecond bimolecular rebinding of CO from the solvent to R state molecules, and a millisecond bimolecular rebinding of CO from solvent to tetramers that have switched to the T quaternary state (*58, 59*). The kinetics is more complex due to the overlapping tertiary and quaternary conformational changes triggered by the ligation state (*59*). The associated lifetime distribution (Figure 5B) exhibits three bands centered at 90 ns, 200 μs, and 6 ms, in good agreement with previously reported data (*59, 60*).

CO rebinding to PEG-Hb^{deoxy} and PEG-Hb^{oxy}, in the absence of IHP, exhibits a lower geminate rebinding amplitude than HbA and an almost negligible T state bimolecular rebinding (Figure 5A). The associated lifetime distributions (Figure 5B) show two major bands centered at ≈ 90 ns and ≈ 200 μs, corresponding to geminate and bimolecular rebinding, respectively. A barely detectable band appears at 10 ms. The amplitude of the band associated with geminate recombination is lower for PEGylated Hbs than in HbA and becomes broader in the case of PEG-Hb^{oxy}. The band centered around 200 μs displays only minimal differences among samples, suggesting that the rate for CO rebinding to R is similar for all samples.

The presence of the allosteric effector IHP leads to a slight decrease in the amplitude of the geminate phase for both PEG-Hb^{deoxy} and PEG-Hb^{oxy} and a concomitant onset of millisecond T state bimolecular rebinding. The comparison of the rebinding kinetics in the absence and presence of IHP for PEG-Hb^{oxy} (Figure 6A) and the corresponding lifetime distributions (Figure 6B) indicates that, in the presence of IHP, the nanosecond and microsecond bands appear to be slightly shifted toward longer times, with the geminate phase becoming a bit smaller, and a clearly distinguishable additional band at ≈ 9 ms. These effects demonstrate for PEG-Hb^{oxy} and, similarly, for PEG-Hb^{deoxy} (data not shown) that the allosteric effectors bias the distribution of molecules toward states with T-like reactivity.

CO rebinding kinetics were measured for 13 and 98 μM PEG-Hb^{deoxy} (Figure 7A). When PEG-Hb^{deoxy} concentration is increased, an additional kinetic phase appears in the millisecond range. Accordingly, three distinct peaks are present in the MEM lifetime distribution (Figure 7B), corresponding to geminate rebinding (100 and 130 ns, at 13 and 98 μM, respectively) and to bimolecular rebinding to R-like structures (230 and 250 μs, at 13 and 98 μM, respectively) and to T-like structures (12 ms at 98 μM; at 13 μM this band is barely detectable and has a maximum at 7 ms). It is worthwhile to notice that the bands become broader when the protein concentration is increased. Analogous results were obtained for PEG-Hb^{oxy} (data not shown).

Variation of the amplitude of the geminate phase and the concomitant increased amplitude of the slow second-order rebinding in the presence of allosteric effectors (Figure 6), increasing protein concentration (Figure 7), and increasing photolysis level (data not shown) indicate that an R to T quaternary conformational change is occurring upon photolysis also for PEG-Hb^{deoxy} and PEG-Hb^{oxy}. However, when compared to rebinding to HbA, the bimolecular rebinding to T-like structures measured for PEG-Hb^{deoxy} and PEG-Hb^{oxy} exhibits a lower amplitude, suggesting that the bias toward a T-like structure is much lower for these products than for HbA due to a higher concentration of the liganded dimers and a slow kinetics of dimer to tetramer association in the unliganded state.

DISCUSSION

PEG-Hb Heterogeneity. The PEGylation procedure yields topologically heterogeneous products because the similar accessibility of the lysine residues (5−7 per Hb chain) reacting with IMT does not allow an absolute selectivity (*34*). In addition, these modifiable sites are not fully saturated by PEG conjugation because the usual HBOC preparation adds only 6−8 PEG per Hb tetramer, which leaves a small fraction of unmodified chains. The MALDI MS analyses carried out on the chains isolated by SDS-PAGE allowed a reliable quantitative determination of unmodified and differently PEGylated chains distribution. The PEG moiety distribution for PEG-Hb^{deoxy} indicates that the bulk of this product (65−70%) consists of tetramers conjugated with a number of PEG chains centered at the value of 6.6 ± 1. Procedures have been developed for the direct coupling to Hb

Table 2. Effects of CO_2 and Cl^- on Oxygen Affinity[a]

species	stripped $p50_b$ (Torr)	n_b	CO_2 $p50_b$(Torr)	n_b	Cl^- $p50_b$(Torr)	n_b
HbA[b]	2.61 ± 0.05	2.36 ± 0.06	4.09 ± 0.02	2.70 ± 0.04	5.15 ± 0.01	3.08 ± 0.02
NEM-Hb	2.23 ± 0.03	2.35 ± 0.04	3.16 ± 0.05	2.28 ± 0.06	4.14 ± 0.05	2.60 ± 0.06
PEG-Hb^{deoxy}	3.18 ± 0.08	2.54 ± 0.19	3.71 ± 0.03	2.21 ± 0.03	3.66 ± 0.05	2.23 ± 0.06
PEG-Hb^{oxyb}	0.85 ± 0.02	1.34 ± 0.04	1.23 ± 0.03	1.33 ± 0.06	1.38 ± 0.04	1.44 ± 0.06

[a] $p50_b$ of HbA, NEM-Hb, PEG-Hb^{deoxy}, and PEG-Hb^{oxy}, in the absence and presence of physiological concentrations of CO_2 and saturating concentration of Cl^- (200 mM), in a solution containing 100 mM Hepes, 1 mM EDTA, at 15°C, pH 7.0. The sample concentration is 110−200 μM. [b] For HbA and PEG-Hb^{oxy}, p50 and n were obtained by fitting ODCs to a single species.

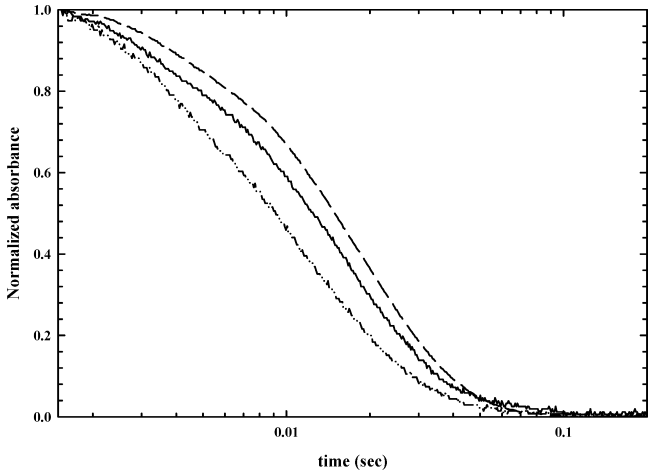

Figure 4. CO binding kinetics to PEG-Hb^{deoxy}, PEG-Hb^{oxy}, and Hb, in the absence of allosteric effectors. Normalized absorbance changes at 435 nm followed upon rapid mixing of deoxy 14 μM PEG-Hb^{oxy} (dash-dot-dot line), 6.6 μM PEG-Hb^{deoxy} (solid line), and 3.5 μM HbA (dash line) in a solution containing 100 mM Hepes, 1 mM EDTA, pH 7, 0.5 atm CO at 15 °C.

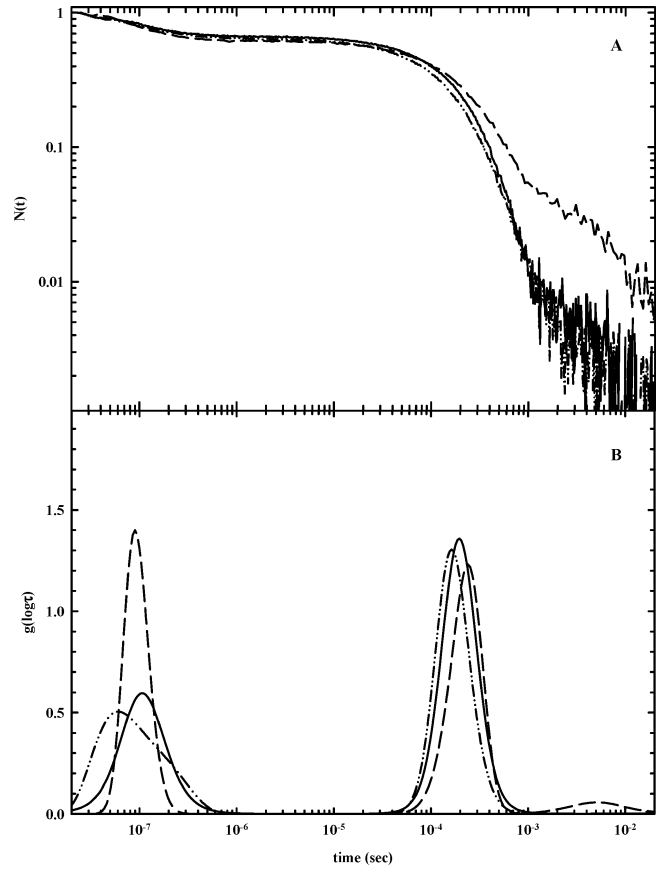

Figure 5. Ligand rebinding kinetics to HbA, PEG-Hb^{deoxy}, and PEG-Hb^{oxy}, after photodissociation of the CO complex. (A) Kinetic progress curves for the fraction of deoxyhemes vs time are reported for HbA (dashed line), PEG-Hb^{deoxy} (solid) and PEG-Hb^{oxy} (dash-dot-dot line) in a solution containing 100 mM Hepes, 1 mM EDTA, pH 7.0, 1 atm CO, at 15 °C, 105 μM HbA, 110 μM PEG-Hb^{deoxy} and 107 μM PEG-Hb^{oxy}. (B) Lifetime distributions associated with the kinetics shown in panel A, calculated using MEM analysis.

of functionalized PEG (*61, 62*). It cannot be excluded that bound bulky PEG molecules steer the attachment of other PEG molecules leading to products less heterogeneous than those obtained in the two-step PEGylation procedure. However, the issue of molecular weight heterogeneity may also concern these products because of the large number of potential attachment sites, 42 lysines and 4 α-amino groups, with respect to the much lower number, 6−8, of bound PEGs. Thus, it seems unavoidable that PEGylated Hb is a heterogeneous product. This relatively wide species heterogeneity leads to different physicochemical and physiological properties that should be taken into account when in vivo experiments are analyzed and might be responsible for some of the observed adverse effects (*23*).

PEGylated Hb Tetramer Stability. Native Hb undergoes a reversible tetramer−dimer equilibrium as depicted by eq 4:

$$(\alpha\beta)(\alpha\beta) \underset{k_{ass}}{\overset{k_{diss}}{\rightleftharpoons}} 2(\alpha\beta) \qquad (4)$$

where $(\alpha\beta)(\alpha\beta)$ represents the tetrameric form and $(\alpha\beta)$ the dimeric form of the protein.

The rate of dissociation, k_{diss}, is ligation-dependent with $k_{diss(deoxy)} \ll k_{diss(oxy)}$, whereas the rate of association, k_{ass}, is ligation-independent (*37*). The reactions in eq 4 have several important implications for evaluation of the in vitro and in vivo properties of PEGylated Hbs: (i) the exchange of dimers among species differing in the number and distribution of conjugated PEG-Hb yields hybrid species. This phenomenon could contribute in vitro to smoothing out the molecular weight heterogeneity of the species and their properties in solution, such as oxygen affinity, allosteric effects, redox potential; (ii) in the circulation, at the interface with tissues, selective permeation of some species may occur leading to a change in the bulk properties of the PEGylated species confined in the plasma; (iii) the order of magnitude of the equilibrium constants for the dissociation of deoxy Hb and oxy Hb are 10^{-11} and 10^{-6} M, respectively. Most Hb mutants with increased oxygen affinity and decreased cooperativity show an increase in $k_{diss(deoxy)}$, although a few cases are known in which an increase in $k_{diss(oxy)}$ has also been observed (*36, 37*). Since the tetramer−dimer equilibrium is an oxygen-linked property, it could be involved in the cooperativity reduction of PEGylated Hbs, mimicking mutant species. A direct study of the reactions in eq 4 by various methods, such as haptoglobin binding (*63*) and hybridization techniques (*64, 65*) was not feasible due to the interference of conjugated PEG.

The equilibrium gel permeation study of NES-Hb showed that the product exhibits the same $K_{diss(oxy)}$ as normal Hb. The $K_{diss(deoxy)}$ value could not be measured because the product was not significantly dissociated under the most dilute conditions, as known for normal Hb. The various PEGylated species in the polydisperse solution of PEG-BSA were not resolved by size

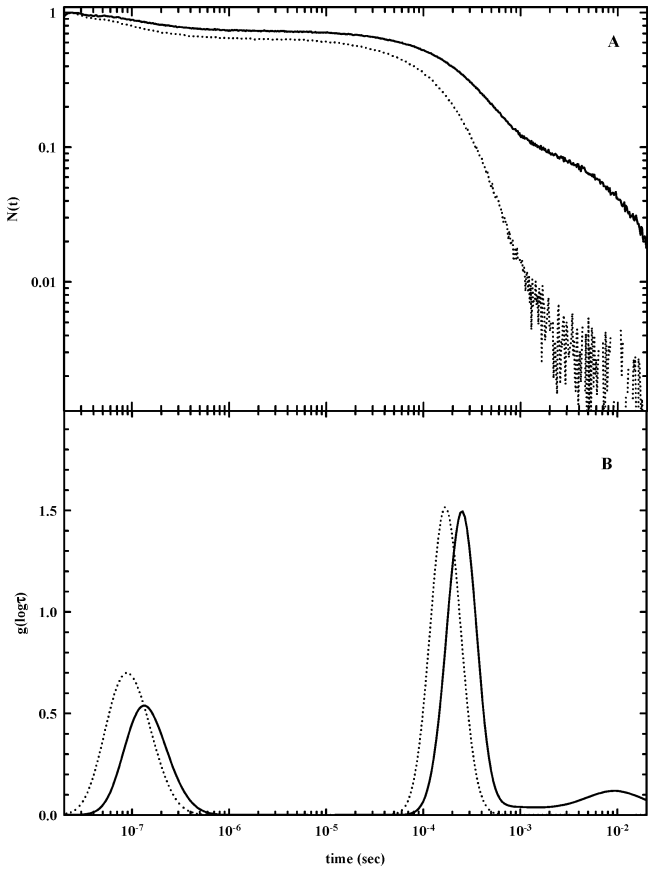

Figure 6. Effect of IHP on PEG-Hb^{oxy} CO rebinding kinetics. (A) CO rebinding kinetics in 100 mM Hepes, 1 mM EDTA, pH 7.0, 1 atm CO, 15 °C, to PEG-Hb^{ox} in the absence (dotted line) and presence (solid line) of 10 mM IHP, at 107 and 100 μM PEG-Hb^{oxy}, respectively. (B) Lifetime distributions associated with the kinetic traces shown in A, calculated using MEM analysis.

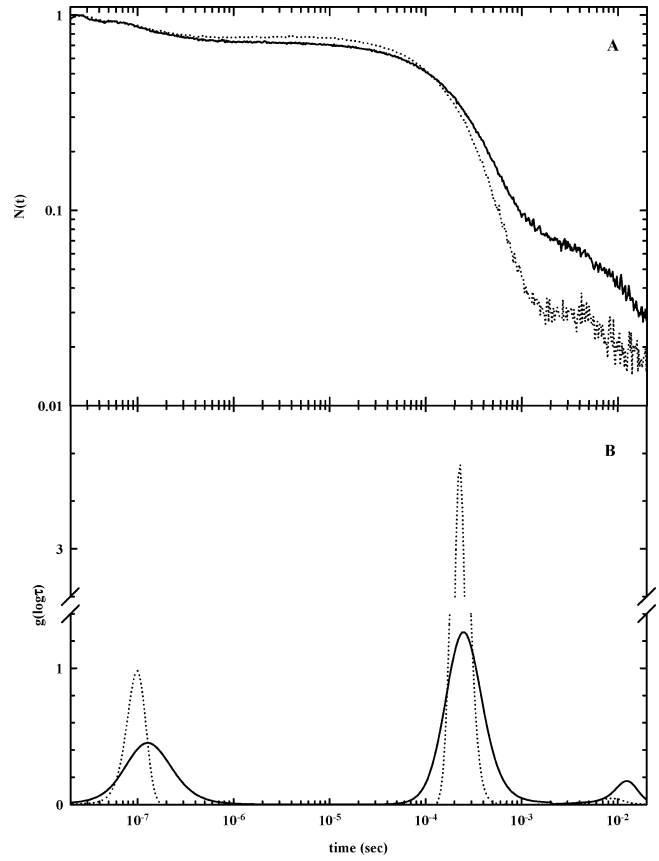

Figure 7. Effect of protein concentration on PEG-Hb^{deoxy} CO rebinding kinetic. (A) CO rebinding kinetics to PEG-Hb^{deoxy} at 13 μM (dotted line) and 98 μM (solid line), 10 mM IHP, 100 mM Hepes, 1 mM EDTA, pH 7.0, 1 atm CO, 15 °C. (B) Lifetime distributions associated with the kinetic traces, shown in A, calculated using MEM analysis.

exclusion chromatography both at high and low product concentration, at which trailing was completely absent. On the contrary, PEG-Hb^{deoxy} under aerobic conditions was resolved into a multiplicity of components upon similar dilution, in agreement with the electrophoretic pattern under native conditions (data not shown). Some of these components had apparent molecular weights consistent with monomeric PEGylated species. Since the phenomenon was completely reversible, the most plausible interpretation is that oxy PEG-Hb^{deoxy} dissociates rapidly into dimers as normal oxy HbA does, but the PEGylated subunits reassociate at a low rate compared with the time scale of the chromatography, in contrast with oxy HbA behavior. This interpretation is consistent with the observation that the slight residual trailing under deoxy conditions was minimal when the sample was obtained by dilution of a deoxygenated solution in which the low molecular weight species had not been given enough time to form (Figure 2B, dashed line). When deoxygenation was carried out rapidly by the addition of dithionite to the diluted oxygenated solution, trailing was more significant because some of the low molecular weight species had not been given enough time to reassociate (Figure 2B, solid line). Two possible explanations for this behavior are the slower translational/rotational coefficient of the PEGylated dimeric species, as suggested by the DLS measurements in dilute solution, also reported by other authors (*32, 66*), and steric interference by PEG in the mechanism of subunit reassociation. The PEG-Hb^{deoxy} chromatography under anaerobic conditions did not show a multiplicity of components. The slight trailing observed at high concentration was not significantly increased upon dilution. This can be attributed to the very slow rate of dissociation of the various PEGylated tetramers as compared with the elution rate.

The size exclusion chromatography studies indicate that under aerobic conditions PEG-Hb^{oxy} was more markedly dissociated into dimers than PEG-Hb^{deoxy} and, under anaerobic conditions, a more pronounced trailing was observed if deoxygenation was achieved by dithionite addition to dilute oxy PEG-Hb^{oxy} (Figure 2C). Fully in keeping with this finding, functional properties of PEG-Hb^{oxy} were found to be less affected by dilution than PEG-Hb^{deoxy} (see below). Therefore, PEGylation carried out under aerobic conditions favors the modification of sites crucial for function and tetramer assembly, likely leading to a very large population of dimeric species. These sites are less severely modified in the anaerobic procedure for PEG-Hb^{deoxy} preparation.

Oxygen Binding Affinity and CO Binding Rate, in the Absence and Presence of Allosteric Effectors. The concentration dependence of the oxygen affinity of PEG-Hb^{deoxy} (Figure 3) and the corresponding analysis (Figure 3, inset) indicates that at least two species are in equilibrium in solution. On the basis of the p50s, Hill coefficients, and responses to allosteric effectors, the more straightforward interpretation is that one species corresponds to PEG-Hb tetramers, characterized by functional properties close to native HbA and the other corresponds to PEG-Hb dimers because its amount increases on dilution. It is interesting to note that the latter species exhibits functional properties very similar to PEG-Hb^{oxy}, that as demonstrated by native electrophoresis and ODC is likely to be composed of heterogeneous highly reactive dimeric species. An alternative interpretation is that the high oxygen affinity species is associated to a perturbed R state tetramer in which the

quaternary transition is either prevented or dramatically slowed down by PEGylation. Such an interpretation is consistent with the hypothesis suggested by Svergun et al. (*33*) that PEG chains may interfere with the T/R transition by binding at the dimer interface, thereby reducing cooperativity. However, the ODC dependence on concentration favors the former interpretation.

PEG-Hb^{deoxy} more than PEG-Hb^{oxy} responds to the physiological concentrations of CO_2 and Cl^- by reducing the oxygen affinity, although not to the same extent as native HbA (Table 2). This can be explained since one of the binding sites common to both ligands involves the α-amino groups of the α chains. PEGylation of Lysα7 likely interferes with the salt bridge formed by Valα1 and removes part of the oxygen-linked CO_2, Cl^-, and Bohr effects involving this site (*34, 67*). However, the protection of the 2,3-BPG binding pocket during PEGylation for PEG-Hb^{deoxy}, but not PEG-Hb^{oxy}, allows CO_2 modulation through binding in the deoxy structure to the amino groups of Val1β, the major site of CO_2 binding (*68*), and Cl^- modulation through binding to Lysβ82 (*69*). These data support the notion that PEGylation of deoxy Hb exhibits a less dramatic impact on protein functional properties.

The comparison of CO binding and rebinding kinetics of PEG-Hb^{deoxy}, PEG-Hb^{oxy}, and HbA, at high and low concentration, in the absence and presence of IHP, allows further identification of functional differences, associated with distinct species. First, it is interesting to note that CO binding to deoxy PEG-Hb^{deoxy} and PEG-Hb^{oxy} is monophasic, lacks the autocatalytic process typical of native Hb, and is concentration-independent over about a 10-fold range of concentrations (10−100 μM). In particular, the observed rate constant for PEG-Hb^{deoxy} exhibits the same value of the rate associated with the slow phase of HbA, whereas the rate constant for CO binding to PEG-Hb^{oxy} is higher but still lower than the rate of the fast phase observed for HbA. These findings suggest that (i) deoxy PEG-Hb^{deoxy} is predominantly present as T state tetramers converting to the R state slower than CO binding, and (ii) deoxy PEG-Hb^{oxy} is present as a mixture of perturbed dimers and T state tetramers, in keeping with the chromatographic measurements, that slowly are converted to the R state. A more detailed analysis is hampered by the fast rate of reaction, leading to the loss of a significant portion of the kinetic traces. Nevertheless, these data provide complementary information with respect to the more robust results generated from flash photolysis experiments. It was found that CO rebinding to both PEGylated samples, in the absence of IHP, did not show significant bimolecular rebinding to T state. This can be explained by either PEGylation reducing the rate of the R to T quaternary transition or the liganded PEGylated Hbs being predominantly present as dimers that, upon deligation, form T state tetramers on a time scale slower than CO rebinding. The reduced amplitude of the geminate rebinding indicates a faster escape to solvent, as observed in myoglobin. The appearance of milliseconds bimolecular rebinding in the presence of IHP, at higher concentrations or higher pulse energy, clearly signals an increased accumulation of T state tetramers. However, their amount is much lower than in native Hb due to a slow quaternary R to T transition and/or dimer association upon deligation.

In a recent paper, CO binding kinetics was measured for Hemospan (*70*), observing a CO rebinding lacking the geminate phase. This discrepancy with respect to our laser flash photolysis data is most probably due to the instrumental setup used in the previous work that did not allow detection of submicrosecond processes.

Overall, results indicate that PEG-Hb^{oxy} is predominantly in a highly reactive state, characterized by high oxygen affinity and a high rate of CO binding. Ligand binding triggers the formation of dimers faster than the quaternary T to R transition. The same picture holds for PEG-Hb^{deoxy}, assuming that the PEG-Hb^{deoxy} tetrameric T state is more stable than PEG-Hb^{oxy} and the T to R quaternary transition efficiently competes with tetramer dissociation. Thus, under physiological conditions, PEG-Hb^{oxy} and PEG-Hb^{deoxy}, in spite of containing the same average number of PEG molecules, are expected to deliver different amounts of oxygen, react with NO and nitrite with different rates, and trigger different regulatory signals because they exhibit distinct functional and structural properties.

CONCLUSIONS

PEGylation affects Hb in distinct ways: (i) perturbation of the T and R states (*31*), (ii) perturbation of the quaternary transitions (*33*), and (iii) influence on the tetramer−dimer equilibrium (*38*). Although animal studies carried out using PEG-Hb^{deoxy} and other similar products showed only moderately adverse pressure and renal filtration effects in the short period (2−3 h), the long-term effects of the stability upon dilution of the various PEGylated tetramers and dimers should be considered with regard to both the physicochemical and physiological properties of the bulk product in the circulation. The observed anomalous equilibrium of the PEGylated tetramers and product heterogeneity should also be considered in the evaluation of the extravasation and renal filtration behavior of these HBOCs. In view of the reported adverse effects of most HBOCs (*23*), it is mandatory to tightly link functional and structural HBOC properties with biochemical and physiological parameters, including proteomic analyses, associated to organ damages, oxidative stress, and inflammatory signals. This is our long-term ongoing challenge.

ACKNOWLEDGMENT

This work was supported by grant COFIN (programmi di ricerca cofinanziati) 2003 from the MiUR (Ministero dell'Istruzione, dell'Università e della Ricerca Scientifica) to M.P., a grant (LSHB-CT-2004-505023) from the European Union Sixth Framework STREP (Specific Targeted Research Project) to M.P. and A.M. and a grant from Fondazione Cariparma to A.M. We are grateful to the Interdepartmental Measurement Center (CIM), University of Parma, for the use of MALDI-TOF.

LITERATURE CITED

(1) Campanini, B., Bruno, S., Raboni, S., and Mozzarelli, A. (2003) Oxygen Delivery by Allosteric Effectors of Hemoglobin, Blood Substitutes, and Plasma Expanders, in *Cardiovascular Agents and Endocrines* (Abraham, D. J., Ed.) pp 385−442, John Wiley and Sons, Inc., New York.
(2) Winslow, R. M. (2006) *Blood Substitutes*, Elsevier, Amsterdam.
(3) Chang, T. M. S. (1997) *Blood Substitutes - Principles, Methods, Products & Clinical Trials*, Karger, S., Publisher Inc., Basel.
(4) Mozzarelli, A. (2008) Hemoglobin-based oxygen carriers as blood substitutes. *Biochim. Biophys. Acta 1784*, 1363–1364.
(5) Morisaki, H., and Sibbald, W. J. (2004) Tissue oxygen delivery and the microcirculation. *Crit. Care Clin. 20*, 213–223.
(6) Sakai, H., and Tsuchida, E. (2006) Performances of PEG-modified hemoglobin-vesicles as artificial oxygen carriers in microcirculation. *Clin. Hemorheol. Microcirc. 34*, 335–40.
(7) Linberg, R., Conover, C. D., Shum, K. L., and Shorr, R. G. (1998) Increased tissue oxygenation and enhanced radiation sensitivity of solid tumors in rodents following polyethylene glycol conjugated bovine hemoglobin administration. *In Vivo 12*, 167–73.
(8) Teicher, B. A., Holden, S. A., Ara, G., Herman, T. S., Hopkins, R. E., and Menon, K. (1992) Effect of a bovine hemoglobin preparation (SBHS) on the response of two murine solid tumors to radiation therapy or chemotherapeutic alkylating agents. *Biomater. Artif. Cells Immobil. Biotechnol. 20*, 657–60.

(9) Dani, C., Martelli, E., Bertini, G., Pezzati, M., Rossetti, M., Buonocore, G., Paffetti, P., and Rubaltelli, F. F. (2004) Effect of blood transfusions on oxidative stress in preterm infants. *Arch. Dis. Child Fetal Neonatal. Ed. 89*, F408–11.

(10) Chatterjee, R., Welty, E. V., Walder, R. Y., Pruitt, S. L., Rogers, P. H., Arnone, A., and Walder, J. A. (1986) Isolation and characterization of a new hemoglobin derivative cross-linked between the alpha chains (lysine 99 alpha 1–lysine 99 alpha 2). *J. Biol. Chem. 261*, 9929–37.

(11) Vandegriff, K. D., Medina, F., Marini, M. A., and Winslow, R. M. (1989) Equilibrium oxygen binding to human hemoglobin cross-linked between the alpha chains by bis(3,5-dibromosalicyl) fumarate. *J. Biol. Chem. 264*, 17824–33.

(12) Cheng, D. C., Mazer, C. D., Martineau, R., Ralph-Edwards, A., Karski, J., Robblee, J., Finegan, B., Hall, R. I., Latimer, R., and Vuylsteke, A. (2004) A phase II dose-response study of hemoglobin raffimer (Hemolink) in elective coronary artery bypass surgery. *J. Thorac. Cardiovasc. Surg. 127*, 79–86.

(13) Hughes, G. S., Jr., Antal, E. J., Locker, P. K., Francom, S. F., Adams, W. J., and Jacobs, E. E., Jr. (1996) Physiology and pharmacokinetics of a novel hemoglobin-based oxygen carrier in humans. *Crit. Care Med. 24*, 756–64.

(14) Sehgal, L. R., Gould, S. A., Rosen, A. L., Sehgal, H. L., and Moss, G. S. (1984) Polymerized pyridoxylated hemoglobin: a red cell substitute with normal oxygen capacity. *Surgery 95*, 433–8.

(15) Iwashita, Y., Yabuki, A., Yamaji, K., Iwasaki, K., Okami, T., Hirata, C., and Kosaka, K. (1988) A new resuscitation fluid "stabilized hemoglobin" preparation and characteristics. *Biomater. Artif. Cells Artif. Organs 16*, 271–80.

(16) Vandegriff, K. D., Malavalli, A., Wooldridge, J., Lohman, J., and Winslow, R. M. (2003) MP4, a new nonvasoactive PEG-Hb conjugate. *Transfusion 43*, 509–516.

(17) Conover, C. D., Malatesta, P., Lejeune, L., Chang, C. L., and Shorr, R. G. (1996) The effects of hemodilution with polyethylene glycol bovine hemoglobin (PEG-Hb) in a conscious porcine model. *J. Invest. Med. 44*, 238–46.

(18) Nho, K., Linberg, R., Johnson, M., Gilbert, C., and Shorr, R. (1994) PEG-hemoglobin: an efficient oxygen-delivery system in the rat exchange transfusion and hypovolemic shock models. *Artif. Cells Blood Substit. Immobil. Biotechnol. 22*, 795–803.

(19) Jahr, J. S., Moallempour, M., and Lim, J. C. (2008) HBOC-201, hemoglobin glutamer-250 (bovine), Hemopure(R) (Biopure Corporation). *Exp. Opin. Biol. Ther. 8*, 1425–1433.

(20) Smani, Y. (2008) Hemospan: a hemoglobin-based oxygen carrier for potential use as a blood substitute and for the potential treatment of critical limb ischemia. *Curr. Opin. Invest. Drugs 9*, 1009–19.

(21) Levy, J. H., Goodnough, L. T., Greilich, P. E., Parr, G. V., Stewart, R. W., Gratz, I., Wahr, J., Williams, J., Comunale, M. E., Doblar, D., Silvay, G., Cohen, M., Jahr, J. S., and Vlahakes, G. J. (2002) Polymerized bovine hemoglobin solution as a replacement for allogeneic red blood cell transfusion after cardiac surgery: results of a randomized, double-blind trial. *J. Thorac. Cardiovasc. Surg. 124*, 35–42.

(22) Olofsson, C., Ahl, T., Johansson, T., Larsson, S., Nellgard, P., Ponzer, S., Fagrell, B., Przybelski, R., Keipert, P., Winslow, N., and Winslow, R. M. (2006) A multicenter clinical study of the safety and activity of maleimide-polyethylene glycol-modified Hemoglobin (Hemospan) in patients undergoing major orthopedic surgery. *Anesthesiology 105*, 1153–63.

(23) Natanson, C., Kern, S. J., Lurie, P., Banks, S. M., and Wolfe, S. M. (2008) Cell-free hemoglobin-based blood substitutes and risk of myocardial infarction and death: a meta-analysis. *J. Am. Med. Assoc. 299*, 2304–12.

(24) Greenburg, A. G., Pitman, A., Pearce, B., and Kim, H. W. (2008) Clinical contextualization and the assessment of adverse events in HBOC trials. *Artif. Cells Blood Substit. Immobil. Biotechnol. 36*, 477–486.

(25) Young, M. A., Lohman, J., Malavalli, A., Vandegriff, K. D., Winslow, R. M. (2009) Hemospan improves outcome in a model of perioperative hemodilution and blood loss in the rat: comparison with hydroxyethyl starch. *J. Cardiothorac. Vasc. Anesth. 23*, 339–347.

(26) Vandegriff, K. D., Malavalli, A., Mkrtchyan, G. M., Spann, S. N., Baker, D. A., and Winslow, R. M. (2008) Sites of modification of hemospan, a poly(ethylene glycol)-modified human hemoglobin for use as an oxygen therapeutic. *Bioconjugate Chem. 19*, 2163–2170.

(27) Olofsson, C., Nygards, E. B., Ponzer, S., Fagrell, B., Przybelski, R., Keipert, P. E., Winslow, N., and Winslow, R. M. (2008) A randomized, single-blind, increasing dose safety trial of an oxygen-carrying plasma expander (Hemospan) administered to orthopaedic surgery patients with spinal anaesthesia. *Transfus. Med. 18*, 28–39.

(28) Jia, L., Bonaventura, C., Bonaventura, J., and Stamler, J. S. (1996) S-nitrosohaemoglobin: a dynamic activity of blood involved in vascular control. *Nature 380*, 221–6.

(29) Pawloski, J. R., Hess, D. T., and Stamler, J. S. (2001) Export by red blood cells of nitric oxide bioactivity. *Nature 409*, 622–6.

(30) Stamler, J. S., Jia, L., Eu, J. P., McMahon, T. J., Demchenko, I. T., Bonaventura, J., Gernert, K., and Piantadosi, C. A. (1997) Blood flow regulation by S-nitrosohemoglobin in the physiological oxygen gradient. *Science 276*, 2034–7.

(31) Lui, F. E., Dong, P., and Kluger, R. (2008) Polyethylene glycol conjugation enhances the nitrite reductase activity of native and cross-linked hemoglobin. *Biochemistry 47*, 10773–80.

(32) Manjula, B. N., Tsai, A., Upadhya, R., Perumalsamy, K., Smith, P. K., Malavalli, A., Vandegriff, K., Winslow, R. M., Intaglietta, M., Prabhakaran, M., Friedman, J. M., and Acharya, A. S. (2003) Site-specific PEGylation of hemoglobin at Cys-93(beta): correlation between the colligative properties of the PEGylated protein and the length of the conjugated PEG chain. *Bioconjugate Chem. 14*, 464–72.

(33) Svergun, D. I., Ekstrom, F., Vandegriff, K. D., Malavalli, A., Baker, D. A., Nilsson, C., and Winslow, R. M. (2008) Solution structure of poly(ethylene) glycol-conjugated hemoglobin revealed by small-angle X-ray scattering: implications for a new oxygen therapeutic. *Biophys. J. 94*, 173–81.

(34) Iafelice, R., Cristoni, S., Caccia, D., Russo, R., Rossi-Bernardi, L., Lowe, K. C., and Perrella, M. (2007) Identification of the sites of deoxyhaemoglobin PEGylation. *Biochem. J. 403*, 189–196.

(35) Portoro, I., Kocsis, L., Herman, P., Caccia, D., Perrella, M., Ronda, L., Bruno, S., Bettati, S., Micalella, C., Mozzarelli, A., Varga, A., Vas, M., Lowe, K. C., and Eke, A. (2008) Towards a novel haemoglobin-based oxygen carrier: Euro-PEG-Hb, physico-chemical properties, vasoactivity and renal filtration. *Biochim. Biophys. Acta 1784*, 1402–1409.

(36) LiCata, V. J., Speros, P. C., Rovida, E., and Ackers, G. K. (1990) Direct and indirect pathways of functional coupling in human hemoglobin are revealed by quantitative low-temperature isoelectric focusing of mutant hybrids. *Biochemistry 29*, 9771–83.

(37) Turner, G. J., Galacteros, F., Doyle, M. L., Hedlund, B., Pettigrew, D. W., Turner, B. W., Smith, F. R., Moo-Penn, W., Rucknagel, D. L., and Ackers, G. K. (1992) Mutagenic dissection of hemoglobin cooperativity: effects of amino acid alteration on subunit assembly of oxy and deoxy tetramers. *Proteins 14*, 333–50.

(38) Hu, T., Li, D., Manjula, B. N., Brenowitz, M., Prabhakaran, M., and Acharya, S. A. (2009) PEGylation of Val-1(alpha) destabilizes the tetrameric structure of hemoglobin. *Biochemistry 48*, 608–16.

(39) Ampulski, R. S., Ayers, V. E., and Morell, S. A. (1969) Determination of the reactive sulfhydryl groups in heme proteins with 4,4′-dipyridinedisulfide. *Anal. Biochem. 32*, 163–9.

(40) Laemmli, U. K. (1970) Cleavage of structural proteins during the assembly of the head of bacteriophage T4. *Nature 227*, 680–5.

(41) Cantu, L., Corti, M., Lago, P., Musolino, M. (1991) In *Photon Correlation Spectroscopy: Multicomponent Systems* (Kenneth, S. S., Ed.) pp 144−159, SPIE, Los Angeles.

(42) Degiorgio, V., Corti, M., and Minero, C. (1984) Laser light scattering in micellar solutions. *Il Nuovo Cimento D 3*, 44–61.

(43) Winzor, D. J., and Scheraga, H. A. (1963) Studies of chemically reacting systems on Sephadex. I. Chromatographic demonstration of the Gilbert theory. *Biochemistry 2*, 1263–1267.

(44) Hayashi, A., Suzuki, T., and Shin, M. (1973) An enzymic reduction system for metmyoglobin and methemoglobin, and its application to functional studies of oxygen carriers. *Biochim. Biophys. Acta 310*, 309–16.

(45) Ronda, L., Bruno, S., Faggiano, S., Bettati, S., and Mozzarelli, A. (2008) Oxygen binding to heme proteins in solution, encapsulated in silica gels, and in the crystalline state. *Methods Enzymol. 437*, 311–28.

(46) Bettati, S., and Mozzarelli, A. (1997) T state hemoglobin binds oxygen noncooperatively with allosteric effects of protons, inositol hexaphosphate, and chloride. *J. Biol. Chem. 272*, 32050–32055.

(47) Rivetti, C., Mozzarelli, A., Rossi, G. L., Henry, E. R., and Eaton, W. A. (1993) Oxygen binding by single crystals of hemoglobin. *Biochemistry 32*, 2888–2906.

(48) Abbruzzetti, S., Bruno, S., Faggiano, S., Ronda, L., Grandi, E., Mozzarelli, A., and Viappiani, C. (2008) Characterization of ligand migration mechanisms inside hemoglobins from the analysis of geminate rebinding kinetics. *Methods Enzymol. 437*, 329–45.

(49) Abbruzzetti, S., Bruno, S., Faggiano, S., Grandi, E., Mozzarelli, A., and Viappiani, C. (2006) Time-resolved methods in Biophysics. 2. Monitoring haem proteins at work with nanosecond laser flash photolysis. *Photochem. Photobiol. Sci. 5*, 1109–20.

(50) Steinbach, P. J. (1996) Two-dimensional distributions of activation enthalpy and entropy from kinetics by the maximum entropy method. *Biophys. J. 70*, 1521–8.

(51) Sottini, S., Abbruzzetti, S., Spyrakis, F., Bettati, S., Ronda, L., Mozzarelli, A., and Viappiani, C. (2005) Geminate rebinding in R-state hemoglobin: kinetic and computational evidence for multiple hydrophobic pockets. *J. Am. Chem. Soc. 127*, 17427–17432.

(52) Abbruzzetti, S., Giuffrida, S., Sottini, S., Viappiani, C., and Cordone, L. (2005) Light-induced protein-matrix uncoupling and protein relaxation in dry samples of trehalose-coated MbCO at room temperature. *Cell Biochem. Biophys. 43*, 431–7.

(53) Sottini, S., Abbruzzetti, S., Viappiani, C., Ronda, L., and Mozzarelli, A. (2005) Determination of microscopic rate constants for CO binding and migration in myoglobin encapsulated in silica gels. *J. Phys. Chem. B 109*, 19523–8.

(54) Antonini, E. , Brunori, M. (1971) *Hemoglobin and Myoglobin in Their Reactions with Ligands*, Amsterdam.

(55) MacQuarrie, R., and Gibson, Q. H. (1972) Ligand binding and release of an analogue of 2,3-bisphosphoglycerate from human hemoglobin. *J. Biol. Chem. 247*, 5686–5694.

(56) Reisberg, P. I., and Olson, J. S. (1980) Kinetic and cooperative mechanisms of ligand binding to hemoglobin. *J. Biol. Chem. 255*, 4159–4169.

(57) Noble, R. W., Kwiatkowski, L. D., Hui, H. L., Bruno, S., Bettati, S., and Mozzarelli, A. (2002) Correlation of protein functional properties in the crystal and in solution: The case study of T-state hemoglobin. *Protein Sci. 11*, 1845–1849.

(58) Hofrichter, J., Sommer, J. H., Henry, E. R., and Eaton, W. A. (1983) Nanosecond absorption spectroscopy of hemoglobin: elementary processes in kinetic cooperativity. *Proc. Natl. Acad. Sci. U.S.A. 80*, 2235–9.

(59) Henry, E. R., Jones, C. M., Hofrichter, J., and Eaton, W. A. (1997) Can a two-state MWC allosteric model explain hemoglobin kinetics? *Biochemistry 36*, 6511–28.

(60) Goldbeck, R. A., Paquette, S. J., Bjorling, S. C., and Kliger, D. S. (1996) Allosteric intermediates in hemoglobin. 2. Kinetic modeling of HbCO photolysis. *Biochemistry 35*, 8628–39.

(61) Hu, T., Manjula, B. N., Li, D., Brenowitz, M., and Acharya, S. A. (2007) Influence of intramolecular cross-links on the molecular, structural and functional properties of PEGylated haemoglobin. *Biochem. J. 402*, 143–51.

(62) Hu, T., Prabhakaran, M., Acharya, S. A., and Manjula, B. N. (2005) Influence of the chemistry of conjugation of poly(ethylene glycol) to Hb on the oxygen-binding and solution properties of the PEG-Hb conjugate. *Biochem. J. 392*, 555–64.

(63) Thomas, J. O., and Edelstein, S. J. (1972) Observation of the dissociation of unliganded hemoglobin. *J. Biol. Chem. 247*, 7870–4.

(64) Bunn, H. F., and McDonough, M. (1974) Asymmetrical hemoglobin hybrids. An approach to the study of subunit interactions. *Biochemistry 13*, 988–93.

(65) Perrella, M., Samaja, M., and Rossi-Bernardi, L. (1979) Hybrid formation for liganded hemoglobins A and C at subzero temperatures. *J. Biol. Chem. 254*, 8748–50.

(66) Li, D., Manjula, B. N., and Acharya, A. S. (2006) Extension arm facilitated PEGylation of hemoglobin: correlation of the properties with the extent of PEGylation. *Protein J. 25*, 263–74.

(67) Perutz, M. F. (1970) Stereochemistry of cooperative effects in haemoglobin. *Nature 228*, 726–39.

(68) Perrella, M., Kilmartin, J. V., Fogg, J., and Rossi-Bernardi, L. (1975) Identification of the high and low affinity CO2-binding sites of human haemoglobin. *Nature 256*, 759–61.

(69) Nigen, A. M., Manning, J. M., and Alben, J. O. (1980) Oxygen-linked binding sites for inorganic anions to hemoglobin. *J. Biol. Chem. 255*, 5525–9.

(70) Vandegriff, K. D., Young, M. A., Lohman, J., Bellelli, A., Samaja, M., Malavalli, A., and Winslow, R. M. (2008) CO-MP4, a polyethylene glycol-conjugated haemoglobin derivative and carbon monoxide carrier that reduces myocardial infarct size in rats. *Br. J. Pharmacol. 154*, 1649–1661.

BC900130F